INTERNATIONAL JOURNAL OF ENGINEERING SCIENCES & MANAGEMENT

COLOR IMAGE SEGMENTATION USING STATISTICAL FEATURES AND DEMPSTER-SHAFER EVIDENCE THEORY

Rafika Harrabi, Ezzedine Ben Braiek

* ESSTT, CEREP Unit, University of Tunisia

ABSTRACT

In this paper, we propose a new color image segmentation method based on a possibilistic clustering algorithm and data fusion techniques. The general idea of mass functions estimation in the Dempster-Shafer evidence theory is to link, at the image pixel level, the notion of membership in fuzzy logic. For segmentation, we proceed in two steps. In the first step, we begin by identifying the most significant attribute images of the tristimuli (R, G and B) and automatically determining the mass functions. In the second step, the evidence theory is employed to merge several attribute images which characterized the three component images, in order to get a final reliable and accurate segmentation result.

The mass functions assigned to each pixel covered the images to be combined, is obtained from the membership degree of the current pixel and those of its neighboring pixels. The membership degree of each pixel is determined by applying the possibilistic clustering approach to the representative attribute images, and the final segmentation is achieved, on an input image, characterized by different attribute images, by using the DS combination rule and decision.

Experimental segmentation results on medical and textured color images demonstrate the value of introducing the fuzzy clustering combined with the statistical features in the evidence theory for color image segmentation. The obtained results show the robustness of the proposed method.

Keywords: Segmentation, Medical image, conflict, possibilistic clustering approach, Dempster-Shafer evidence theory, data fusion.

INTRODUCTION

Image segmentation is a critical and important basic operation for meaningful and interpretation of image acquired [1] [2], and it's one of the most difficult tasks in image processing, which determines the quality of the final results of analysis. The goal of image segmentation is the partition an image in regions visually distinct and uniform, according to texture, color tone etc … In this frame work, color image segmentation has wide applications in many areas [3] [4], and many different techniques have been developed [5] [6].

In the most of the existing color image segmentation techniques, the definition of a region is based on similar color. Most gray level image segmentation technique can be extended to color images, such as histogram thresholding [7], clustering, regions growing, edge detection [8], fuzzy methods [9] etc., by applying these techniques to each component of the input image expressed in the RGB color space, or their linear/non-linear transformations [10] [11], and then the results can be combined in some way to obtain the final segmentation result.

*Corresponding Author
Email: Refka_esstt@yahoo.fr

Each color representation has its advantages and disadvantages [11] [12]. There is still no color representation that can dominate the others for all kinds of color images yet [13]. The general segmentation problem consists in choosing the adapted color model for a specific application. Nonlinear color transformations such as HIS have essential singularities which are non-removable. The RGB color space is suitable for color display, but not good for color scene segmentation and analysis because of the high correlation among the R, G and B components. By high correlation, we mean that if the intensity changes, all the three components will change accordingly. In this context, image segmentation using data fusion techniques appears to be an interesting method.

Data fusion [4] [14] [15], is a technique which consists to combining information coming from different sources in order to get an optimal set of objects under investigation. The most significant advantage of using data fusion

techniques [14], is to handle uncertain, imprecise and incomplete information, by combining both redundant and complementary data. Over the existing data fusion methods such as evidence theory [15], probability theory [16], fuzzy logic [17], possibility theory [18] etc., the DS evidence theory [19] [20] offers a powerful and flexible mathematical tool for handling uncertain, imprecise and incomplete information. An important property of this theory is its ability to merge different data sources in order to increase the information quality. However, to fuse different informations using evidence theory, the appropriate determination of mass functions plays a crucial role, since assignation of a pixel to a cluster is given directly by the estimated mass functions.

Many authors have addressed this problem using different approaches [21] [22] [23] and several researchers have, in particular, investigated the relationship between the fuzzy sets and the Dempster-Shafer evidence theory [17] [20].

In this context, Zimmerman and Zysmo [24], have shown through empirical studies that the good model of the information representation is based on the distance $distance$ of a point from a prototypical member. However, one of the major factors that influences the determination of the membership functions is the "distance measure" chosen for the problem at hand [23].

Also, Ben Chaabane et al. [4], have proposed a color image segmentation method based on fuzzy homogeneity and Dempster-Shafer evidence theory (HHDS). The general idea of mass function estimation in the Dempster-Shafer evidence theory of the histogram is extended to the homogeneity domain. The authors have shown through empirical studies that a good model of the mass functions estimation in the DS evidence theory is based on the assumption of Gaussian distribution and the homogeneity histogram analysis technique

In particular, several researchers have investigated the relationship between fuzzy sets and DS evidence theory. The advantages provides by fuzzy sets theory are characterized by various definitions of membership functions.

In this context, Min Zhu et al. [20] have been proposed a method of automatically determining the mass functions in the evidence theory. The proposed segmentation (FCMDS) consists in combining several images, together, in order to increase the information quality and to get an optimal segmented image. In the first step, the membership degree of each pixel is determined by applying fuzzy c-means (FCM) clustering to the information coming from the images to be combined. The idea is to link at the image pixel level, the notion of mass functions to that of membership functions in fuzzy logic. In the second step, the evidence theory is employed to merge the input images.

However, FCM algorithm [25] has a considerable difficulty in noisy environments, and the memberships resulting from this algorithm do not always correspond to the intuitive concept of degree of belonging or compatibility. The membership degrees are computed using only gray levels and do not take into account the spatial information of pixels with respect to one another. Also, the Hard C-Means (HCM) [26] is one of the oldest clustering methods in which HCM memberships are hard (i.e., 1 or 0). However, the main differences between the various works cited before occur in the method of mass functions estimation, and in the application.

This paper investigates how the user can choose a suitable method for determining the mass functions in the DS evidence theory. In this work, we shall use the fuzzy sets for estimation the mass functions. So, this work may be seen to be straightforwardly complementary to that in the one proposed by Zhu et al. [20]. Hence, the proposed segmentation method is based on fuzzy sets and data fusion techniques, applied to a specific kind of medical image segmentation, where we aim at providing a help to the doctor for the follow-up of the diseases of the breast cancer. The objective is to rebuild each cell from a series of images. These images are fused together by the evidence theory using as input features, the membership degree previously estimated and associated to each pixel of the representative attribute images extracted from the co-occurrence matrix of each primitive colors (R, G and B). The idea is to link at the image pixel level, the notion of mass functions to that of membership functions by using the Possibilistic C-Means algorithm (PCM) [27]. Once the mass functions are estimated for each attribute images to be fused, the DS combination rule and decision are applied to obtain the final segmented image.

Section 2 introduces a method for the determination of membership degrees. The proposed method for color image segmentation is exposed in Section 3. The experimental results are discussed in Section 4, and the conclusion is given in Section 5.

MATERIALS AND METHODS

Materials

In the medical domain, the doctors follow the diseases of the breast cancer taking into account the number of tumor cells expressing hormone receptor (HR). The assessment of labelled cells expressing the HR can be done on cells in suspension or histological over-part. This latter method is used in the pathology laboratory of cancer center Salah Azaiez in Tunis, Tunisia. The sample preparation is intended to highlight the different cells to be visible.

The cellular structure supports a procedure that requires several steps:

- The fixing is used for the structures conservation and the parts hardening. It must be done immediately after sampling; by immersing the material in an adequate volume of fixative (the fixer used in Salah Institute Azaiez is the formalin at (10%)).
- The inclusion allows realizing the fine and regular cuts. The most commonly used inclusion medium is the paraffin.
- The cuts of the paraffin block are made with a microtome. They allow producing the section slices (thin slices) of 2 μm to 5 μm thick.
- The coloring performed on slides; accentuates the contrasts for the better recognition of the different structure elements. Other colors are intended to highlight specific molecules such as the immunohistochemistry. In our study, the immunohistochemistry coloring is applied to highlighting the hormone receptors.
- The installation: the colored cuts are placed between the blade and the cover slip with a synthetic refractive resin index close to that of glass. Then, a microscopic preparation is obtained ready to be observed with a microscope.
- The acquisition is made by a digital camera NIKON Coolpix 995 mounted on a Nikon E600 microscope that provides a color image in jpg format, with a variable size depending on the desired view field. Although the jpg format is a loss compressed format, but the morphology is preserved and what is of interest to us is the intensity of the dye which has not been significantly changed.

The proposed Method

In this work, we are interested in color image segmentation of cells in the breast images. The problem is to separate cells from the background. The initial segmentation maps which will then be fused together are simply given, in our application, by the Possibilistic C-Means approach [27], applied on the three primitive colors (R, G and B) and using as input the set of pixel values provided by their representative attribute images extracted from the co-occurrence matrix.

The fuzzy sets are used to automatically determination of mass functions in the Dempster-Shafer evidence theory. To do this, the Possibilistic C-Means algorithm (PCM) is applied to each representative attribute images to be fused. Then, the DS combination rule and the decision are applied to obtain the final segmented image. Hence, the main idea of the proposed method is to fuse, one by one, the pixels of the input image characterized by several attribute images.

Determination of membership degrees using PCM

The PCM formulation minimizes the objective function given by:

$$J_m(u,v) = \sum_{k=1}^{n}\sum_{i=1}^{c} u_{ik}^m d_{ik}^2 + \sum_{k=1}^{n}\gamma_k\sum_{i=1}^{c}(1-u_{ik})^m \tag{1}$$

where γ_k are suitable positive numbers.

In Equation 1, d_{ik}^2 is the distance of the feature point x_k to the centers of the classes v_i of an $(N \times M)$ image, $n = M \times N$ is the total number of feature vectors, c is the number of classes that is user dependent and should be known a priori in the PCM algorithm, and $U = [u_{ik}]$ is a $(c \times n)$ matrix, called the fuzzy c-partition matrix [27]. u_{ik} is the membership degree of the feature point x_k in cluster i, and $m \in [1, \infty[$ is a weighting exponent called the fuzzifier.

The necessary conditions on the prototypes are identical to the corresponding conditions in the Fuzzy C-Means (FCM) and its derivatives. Hence minimizing $J_m(u, v)$ with respect to U is equivalent to minimizing the following objective function (1), with respect to each one of the u_{ik} :

$$J_m(u, v) = u_{ik}^m d_{ik}^2 + \gamma_k (1 - u_{ik})^m \qquad (2)$$

Differentiating (2) with respect to u_{ik} and setting it to 0 leads to the equation:

$$u_{ik} = \frac{1}{1 + \left(\frac{d_{ik}^2}{\gamma_k}\right)^{\frac{1}{m-1}}} \qquad (3)$$

Also, it has to be noted that γ_k determines the relative degree to which the second term in the objective function (2) is significant compared to the first term. If both terms are to be weighted roughly equally, then γ_k should depend on d_{ik}^2 with $m = 2$ and:

$$\gamma_k = \frac{\sum_{k=1}^n u_{ik}^m d_{ik}^2}{\sum_{k=1}^n u_{ik}^2} \qquad (4)$$

Hence, the PCM clustering technique can be summarized by the following steps:

- *Fix the number of clusters c.*
- *Fix m; $m > 1$.*
- *Set iteration counter $t = 1$.*
- *Initialize the possibilistic C-partition $U^{(0)}$.*
- *Estimate γ_k using (4)*

Repeat
- *Update the prototypes using $U^{(t)}$, as indicate below.*
- *Compute $U^{(t+1)}$ using (3).*
- *Increment (t).*

Until $\|U^{(t-1)} - U^{(t)}\| < \varepsilon$. *$\varepsilon$ is a chosen positive threshold.*

In the present study, the number of clusters is fixed, the value of m is set to 2, and the clustering process is stopped when $\varepsilon \leq 10^{-5}$.

Spatial information dependence method
The co-occurrence matrix [28], is largely related to the appearance frequency of a pixel couples from an image. It contains significant informations which improve the classes discrimination of an image, so, it plays an important role in image segmentation. The concept of co-occurrence matrix [29], was defined to express the image properties relating to the second order statistics. Here, we have defined the co-occurrence matrix, also called the spatial information dependence method, as the appearance frequency of a pixel couples separated by a distance d, in a particular direction θ.

Assume g_{xy} is the intensity of a pixel p_{xy} at the location (x, y) in an $(M \times N)$ image, W_{xy} is a size $(t \times t)$ window centred at (x, y) for the computation of co-occurrence matrix.
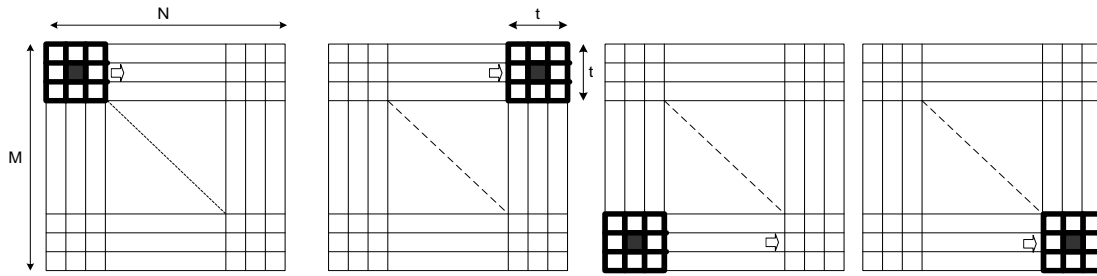
Fig. 1. The adaptive sliding window from left to right and top to bottom on an $(M \times N)$ image.

The window (w_{xy}) is the local regions where the spatial information dependence method is calculated. However, the size of the sliding window has an effect on the computation of the co-occurrence matrix, so on the computation of the statistical features. The window (w_{xy}) should be big enough to allow sufficient information provided to the computation of the statistical features extracted from the co-occurrence matrix. Furthermore, a large window causes a significant processing time. As a trade-off choice, experimentally, a (49×49) window is chosen for computing the co-occurrence matrix.

However, w_{xy} is the local regions where the spatial information dependence method is calculated. So, the co-occurrence matrix describes the appearance frequency of a pixel couples within a local region, and relating to the relation R is calculated for each window (w_{xy}) as follows:

$$Cooc(i,j,R) = card \begin{cases} ((x,y),(x',y')) \in D, & \text{checking } R(d,\theta) \\ I(x,y) = i, & I(x',y') = j \end{cases} \tag{5}$$

Each element of $cooc(i,j,R)$ represents the number of pixels couple (i,j), which denotes how often a pixel with gray-level (grayscale intensity) value i occurs horizontally adjacent to a pixel with the value j in the image. $R(d,\theta)$ is the space relation of the two pixels, with d the distance between the two pixels and $\theta = \{0°,45°,90°,135°\}$ the orientation of the two pixels versus the horizontal.

In our application, the statistical features are extracted from the co-occurrence matrix computed from a sliding window centered around each pixel of the three component images (R, G and B). The spatial scanning order of an image is performed pixel by pixel from left to right and top to bottom, (see Fig. 1). Hence, this technique is used to calculate the new image called the attribute image, (see, Fig. 2).

However, several attributes may be extracted from the co-occurrence matrix such as: Mean $(Mean)$, diagonal moment (DM), contrast $(Cont)$, energy $(Ener)$, directivity $(Direc)$, entropy $(Entr)$, opposite differential moment (ODM), variance (Var), etc.

Let $Cooc(i,j)$ represents the occurring frequency of each pixels couple. It is obtained by calculating how often a pixel with gray-level (grayscale intensity) value i occurs horizontally adjacent to a pixel with the value j in the w_{xy} window. N_c is the maximal gray level pixel value of the sliding window w_{xy}.

Among the statistical attributes used in our application, we can cite: the diagonal moment (DM), the directivity (Direc), the energy (Ener) and the opposite differential moment (ODM), which are given respectively by the following equations:
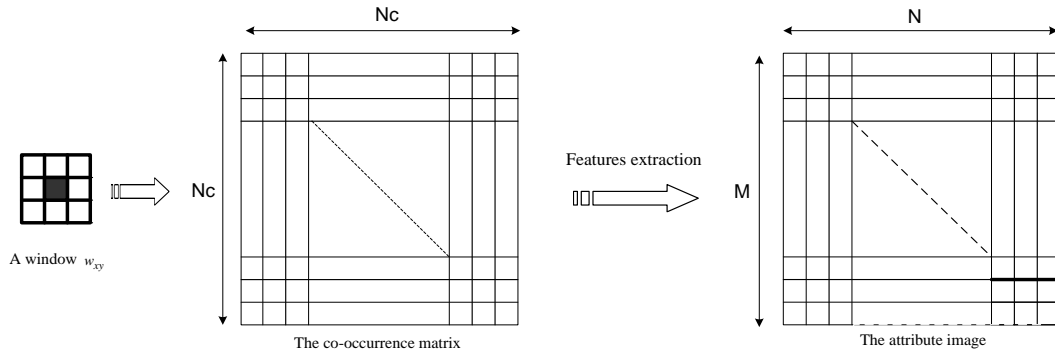
Fig. 2. Features extraction from the co-occurrence matrix using a sliding window.

$$DM = \sum_{i=1}^{Nc} \sum_{j=1}^{Nc} \left(\frac{1}{2} \left(|i - j| \right) Cooc(i,j) \right)^{\frac{1}{2}} \qquad (6)$$

$$Direc = \sum_{i=1}^{Nc} \sum_{j=1}^{Nc} Cooc(i,i) \qquad (7)$$

$$Ener = \sum_{i=1}^{Nc} \sum_{j=1}^{Nc} \left[Cooc(i,j) \right]^2 \qquad (8)$$

$$ODM = \sum_{i=1}^{Nc} \sum_{j=1}^{Nc} \frac{Cooc(i,j)}{1 + (i - j)^2} \qquad (9)$$

where $(N_c \times N_c)$ is the size of the co-occurrence matrix. The size of the co-occurrence matrix is variable according to the maximum value of the intensity in each window.

In this application, we use N=6 attribute images to characterized the input image expressed in RGB color space. The examples show that the informations provided by these different images are redundant and complementary. In this sense, data fusion techniques appear as an appealing approach for color image segmentation.

Use of DS evidence theory for image segmentation
The purpose of this work is to apply this method to a specific kind of medical image segmentation, where we aim at providing a help to the doctor for the follow-up of the diseases of the breast cancer. From an initial segmentation obtained by using the Possibilistic C-Means algorithm applied to the representative attribute images of the tristimuli (R, G and B), one seeks a segmentation which represents as well as possible the cells, in order to give to the doctors a schema of the points really forming part of the cells, as also the number of the cells.

The selection of the best and representative attribute images is based on the segmentation sensitivity criterion [32] [33]. The best attribute images used in our application are the $\{DM, Direc\}; \{DM, Ener\}$ and $\{Ener, ODM\}$

for the R, G and B component images, respectively. To do this, Possibilistic C-Means algorithm is applied to several attribute images of each primitive color and the attribute image with the best segmentation sensitivity is selected in each primitive color.

The purpose of segmentation is to partition the image into homogeneous regions. The idea of using DS evidence theory for image segmentation is to fuse one by one the pixels, of the input image characterized by several attribute images. The PCM algorithm is applied to the six attribute images. Then, the DS combination rule and the decision are applied to obtain the final segmented image.

The Dempster–Shafer evidence theory [4] [20] aims to represent and handle uncertain information. An important property of this theory is its ability to merge different data sources in order to increase the information quality. This theory affect a degree of confidence, which is called the mass function, to all simple and composed hypotheses (set classes C_i in the present case), and to take into account the lack of information.

In the present study, the clusters (C_i) are generated by the PCM algorithm from the frame of discernment Ω composed of n single mutually exclusive hypotheses H_n, which are symbolized by:

$$\Omega = \{H_1, H_2, ..., H_n\} = \{C_i\}, \qquad 1 \le i \le n \tag{10}$$

In the framework of DS evidence theory, the information from each image to be combined is represented by a mass function (m) assigning values in [0, 1] to each subset of the discernment set Ω. The function m is defined from 2^{Ω} to [0, 1] verifying:

$$\begin{cases} m(\phi) = 0 \\ \displaystyle\sum_{A_n \subseteq \Omega} m(A) = 1 \end{cases} \tag{11}$$

If $m(A) > 0$, A is called focal elements.

The main advantage of DS evidence theory is its robustness of combining information coming from Q sources with the DS orthogonal rules [8][15].

The DS combination can be represented for Q information sources by the following orthogonal rule:

$$m(H_i) = m^1(H_i) \oplus m^2(H_i) \oplus ... \oplus m^Q(H_i) \tag{12}$$

where $\oplus$ is the sum of DS orthogonal rules.

Specifically, the combination (called the joint m12) is calculated from the aggregation of two mass functions m1 and m2 associated to information sources S_1 and S_2. Then:

$$\forall H_i \subseteq \Omega, \ m_{12}(H_i) = \frac{1}{1-K} \sum_{A_1 \cap A_2 = H_i} m_1(A_1).m_2(A_2) \tag{13}$$

where, K is defined by [22]:

$$K = \sum_{A_1 \cap A_2 = \phi} m_1(A_1).m_2(A_2) \tag{14}$$

The normalization coefficient K evaluates the conflict between the sources S_1 and S_2. This is determined by summing the products of mass functions of all sets where the intersection is an empty set.

However, to fuse different images using DS theory, the Dempster-Shafer evidence theory, the appropriate determination of mass functions plays a crucial role, since assignation of a pixel to a cluster is given directly by the estimated mass functions. In the present study, the method of generating the mass functions is based on the fuzzy sets. To do this, Possibilistic C-Means (PCM) algorithm [27] is applied to the representative attribute images.

Mass function of simple hypotheses

Masses of simple hypotheses C_i are directly obtained from the membership degree u_{xy} of the pixel level g_{xy}^q at location (x, y) coming from attribute images (information sources) q to cluster i, as follow:

$$m_i(g_{xy}^q) = u_i(g_{xy}^q) \tag{15}$$

where g_{xy}^q is the information of a pixel p_{xy} at the location (x, y) for one of the six informations sources $(q = 1, 2, ..., 6)$.

Mass function of double hypotheses

The mass assigned to a double hypothesis depends on the membership degrees of both the simple hypotheses. In fact, if there is a high ambiguity in assigning a image pixel level g_{xy}^q coming from attribute images q to cluster r or s, that is $|u_r(g_{xy}^q) - u_s(g_{xy}^q)| < \varepsilon_1$, where ε_1 is the thresholding value, then double hypotheses C_{rs} are formed. In the present study, ε_1 was fixed at 0.15.

Once the double hypotheses (composed of two simple hypotheses) are formed, their joint mass is calculated according to the following formula:

$$m_{rs}(g_{xy}^q) = (1 - u_r(g_{xy}^q)).(1 - u_s(g_{xy}^q)) \tag{16}$$

In the case where the double hypotheses C_j are composed of more than two simple hypotheses

$C_j = C_1 \cup C_2 \cup ... \cup C_M$, their joint mass is determined as follows:

$$m_j(g_{xy}^q) = \prod_{i=1}^{M}(1 - u_i(g_{xy}^q)) \qquad (17)$$

Once the mass functions of the six images are estimated, their combination is performed using the orthogonal sum that can be represented as follows:

$$m_i(g_{xy}) = m_i(g_{xy}^1) \oplus m_i(g_{xy}^2) \oplus ... \oplus m_i(g_{xy}^6) \qquad (18)$$
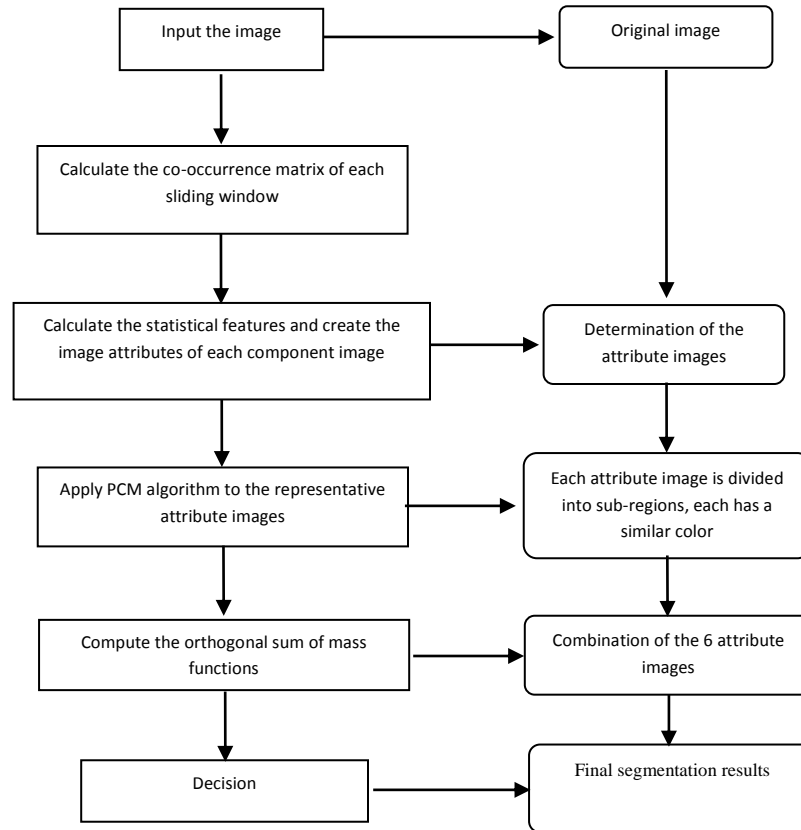

Fig. 3. Flowchart of the proposed method.

Note that this operation is commutative and associative.

After calculating the orthogonal sum of the mass functions for the six features, a decision module is used for labelling each pixel respecting the combined mass functions. The decisional procedure for classification purpose consists in choosing one of the most likely hypotheses C_i. Consequently, the proposed method can be described by a flowchart given in Fig. 3.

EXPERIMENTAL RESULTS

In order to illustrate the methods presented in the previous section, a large variety of medical and synthetic color images are employed in our experiments. The used images data base is shown in Fig. 4.
The images originally are stored in RGB format. Each of the primitive color (red, green and blue) takes 8 bits and has the intensity range from 0 to 255.
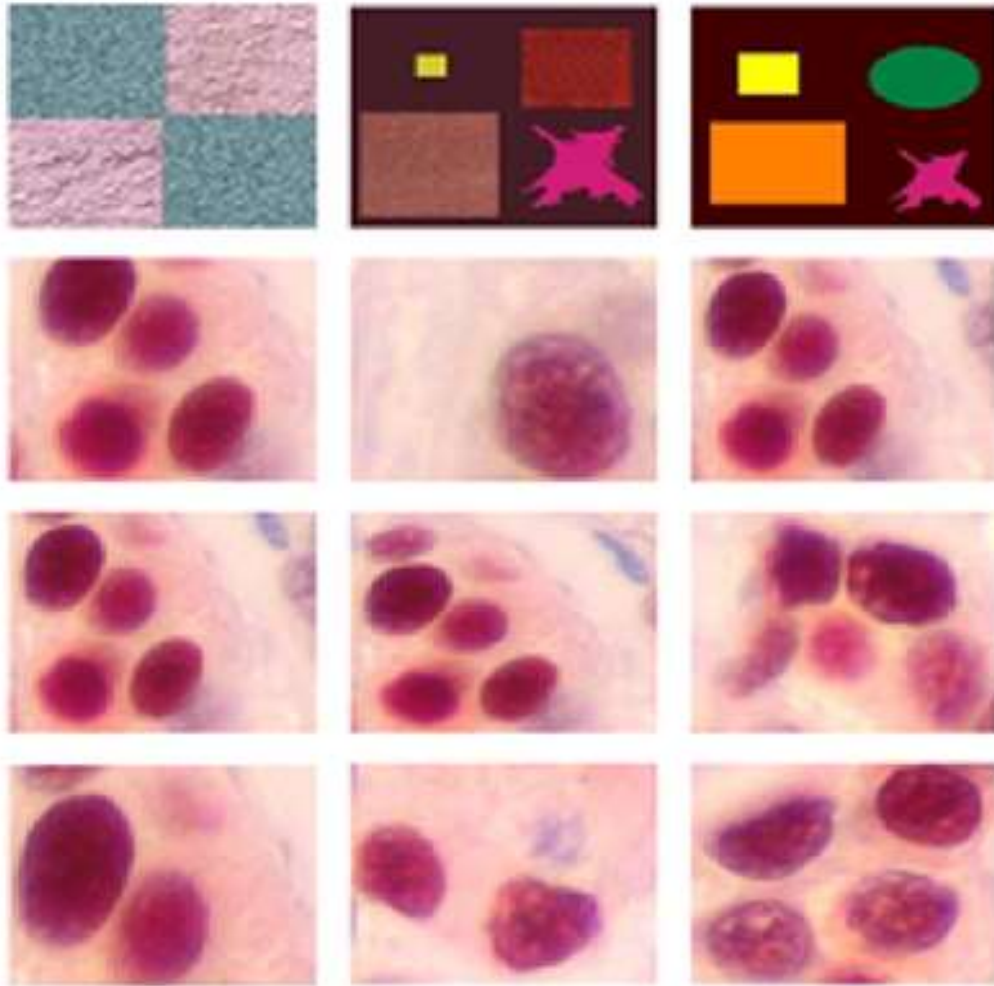
Fig. 4. Data set used in the experiment. Twelve were selected for a comparison study. The patterns are numbered from 1 through 12, starting at the upper left-hand corner.

The first three images presented in Fig.4, represent a synthetic image dataset which is developed and used for numerical evaluation purpose. The nine other images represent real medical cells images, obtained by a himi-histochimy coloring in the Cancer Service previously cited.

In fact, to evaluate the efficiency and accuracy of the proposed edge extraction method, the results are compared versus existing methods, as described earlier. The efficiency evaluations for these different methods are carried out on the Matlab software 7.1.

Fig. 5-7 show the results of the proposed method. Figure 5 shows an example of the possibilistic c-means algorithm applied to the R, G and B components of the image expressed in the RGB color space. The results are shown in Figures 5(b), 5(c), and 5(d). In this case, we find that the resulting images contain some holes and missing features in the cells. Also, the cells are attached, which lead to errors of counting of the number of the cells.
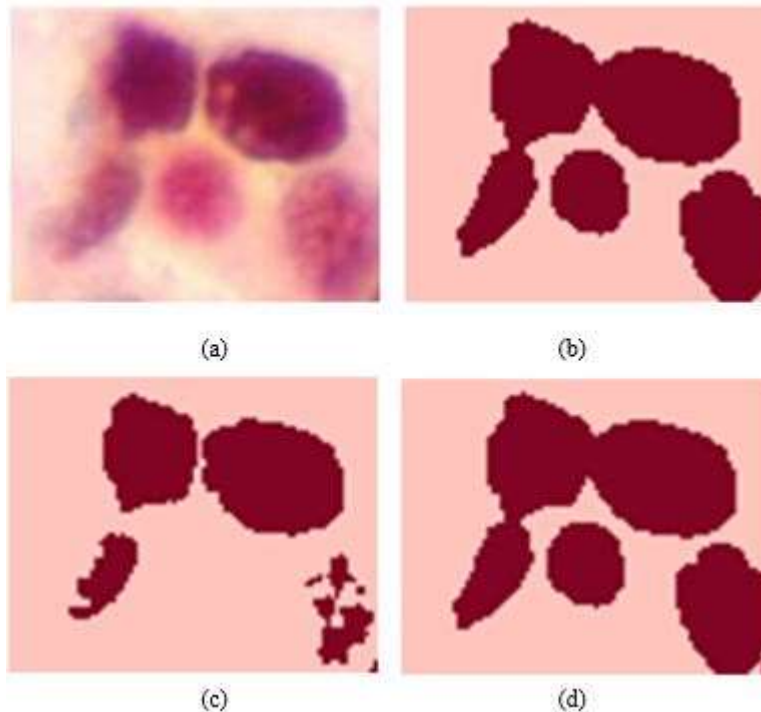
Fig. 5. Segmentation results on a color image. (a) Original image (256×256×3) with gray level spread on the range [0, 255]. (b) Red resulting image by PCM algorithm. (c) Green resulting image by PCM algorithm. (d) Blue resulting image by PCM algorithm.

This shows the lack of information when using only one information source and may be explained by the high degree of correlation among of the three components of the RGB color space. Also, this demonstrates the necessity of using the fusion process.

Also let us compare the performance of our proposed algorithm to those in other published reports that have recently been applied to color images. These include Ben Chaabane et al. [4], Zhu et al. [20], Zimmermann and Zysno [24], Harrabi et al. [30]. The segmentation results are shown in Figures 6, and 7.

Figure 6 shows a comparison of the results between the traditional methods DDS [24], FCMDS [20], HHDS [4] GDDS [30] and the proposed method. The final images using the homogeneity histogram, the FCM algorithm, the distance and the Gaussian distribution for the determination of mass functions in DS theory are shown in Figures 6(b), 6(c), 6(d) and 6(e), respectively. Fig. 6(f) presents the segmentation result based on the propose method.

Comparing the results, we notice that none of them can be considered as reliable except the final segmentation results (at bottom right) which visually identify quite faithfully the different objects of the scene (see Table 1 for an objective and quantitative comparison).

In fact, the experimental results presented in Figure 6(f) are quite consistent with the visualized color distributions in the objects, which make it possible to do an accurate measurement of cell volumes.

Table 1. Segmentation sensitivity From DDS, FCMDS, HHDS and TSMODS for the Data set Shown in Fig. 4

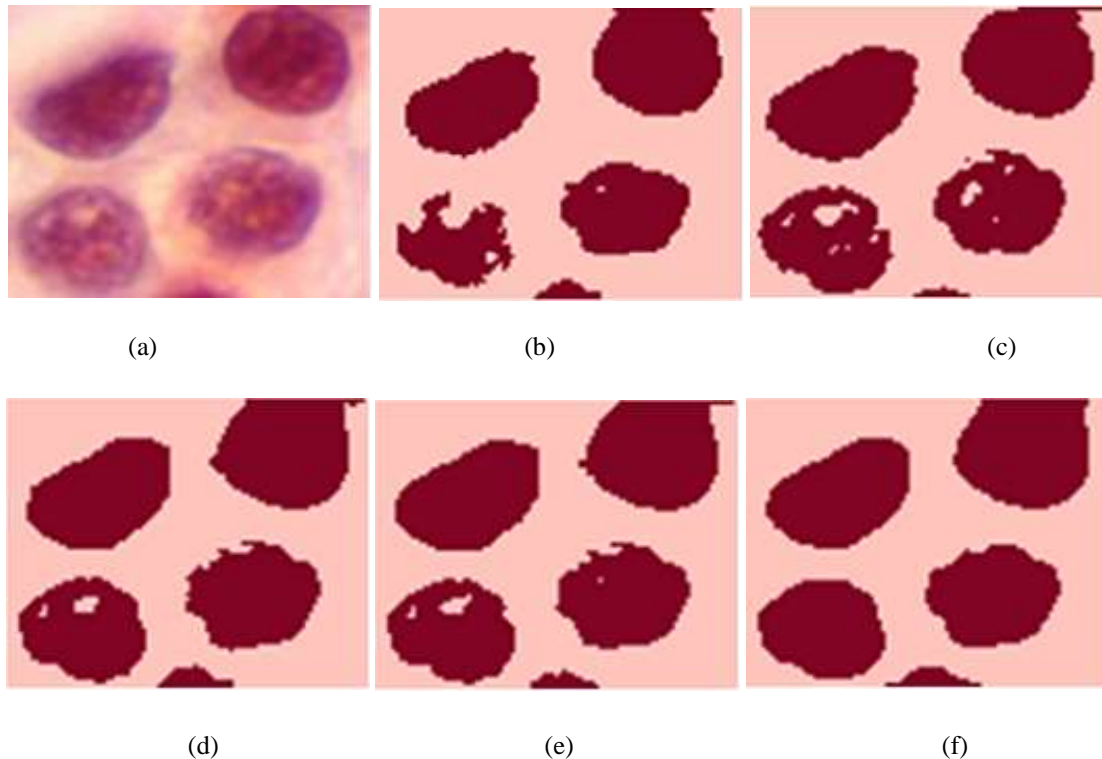|	DDS	FCMDS	HHDS	GDDS	PCMDS (THE PROPOSED METHOD)
	SENSITIVITY SEGMENTATION (%)				
Image 1	0.8252	0.8417	0.9295	0.9667	0.9860
Image 2	0.8214	0.8378	0.9374	0.9749	0.9944
Image 3	0.8125	0.8288	0.9220	0.9589	0.9781
Image 4	0.7537	0.7688	0.9128	0.9493	0.9683
Image 5	0.7705	0.7859	0.9218	0.9587	0.9779
Image 6	0.7802	0.7958	0.9331	0.9704	0.9898
Image 7	0.7496	0.7646	0.9267	0.9638	0.9831
Image 8	0.7915	0.8073	0.9270	0.9641	0.9834
Image 9	0.7964	0.8123	0.9207	0.9575	0.9766
Image 10	0.7639	0.7792	0.9279	0.9650	0.9843
Image 11	0.8109	0.8271	0.9270	0.9641	0.9834
Image 12	0.8056	0.8217	0.9192	0.9560	0.9751

(a) (b) (c)

(d) (e) (f)

Fig. 6. Comparison of the proposed segmentation method with other existing methods on a complex medical image (2 classes, various cells). (a) Original image (256×256×3): color medical image with RGB description, (b) segmentation based on DDS method, (c) segmentation based on GDDS method, (d) segmentation based on HHDS method, (e) segmentation based on FCMDS method, and (f) segmentation based on the propose method.

In short, the proposed algorithm outperforms all these well-known segmentation algorithms in terms of segmentation sensitivity (Sen(%)), see Table 1.

To provide insights into the proposed method, we have compared the performance of the proposed method with those of the corresponding Hard and Fuzzy C-Means algorithms as tools for the estimation of mass functions in the Dempster-Shafer evidence theory. The method was also tested on synthetic images and compared with other existing methods, see Figure 7.

Fig. 7(a) presents the original synthetic image. Fig. 7(b) gives the $(N \times M)$ synthetic image where a "salt and pepper" noise of D density was added. This affects approximately $(D \times (N \times M))$ pixels.

The segmentation results are obtained using the HCM, the FCM and PCM clustering algorithms for the determination of the mass functions in the DS theory. They correspond, respectively, to Figs. 7(c), (d) and (e). Fig. 7(f) gives the reference segmented image.

The improved experimental results have been achieved by the proposed method based on the PCM algorithm which can be used to generate a mass function that has a typical interpretation, that is, the resulting partition of the data can be interpreted as the compatibilities of the points with the class prototypes, while the HCM and FCM methods use only the gray level to determine the degree of membership of each pixel.

Comparing Figures 7(c), 7(d), and 7(e), one can see that the different objects of the image are much better segmented in (e) than those in (c) and (d).

(a)   (b)   (c)

(d)   (e)   (f)
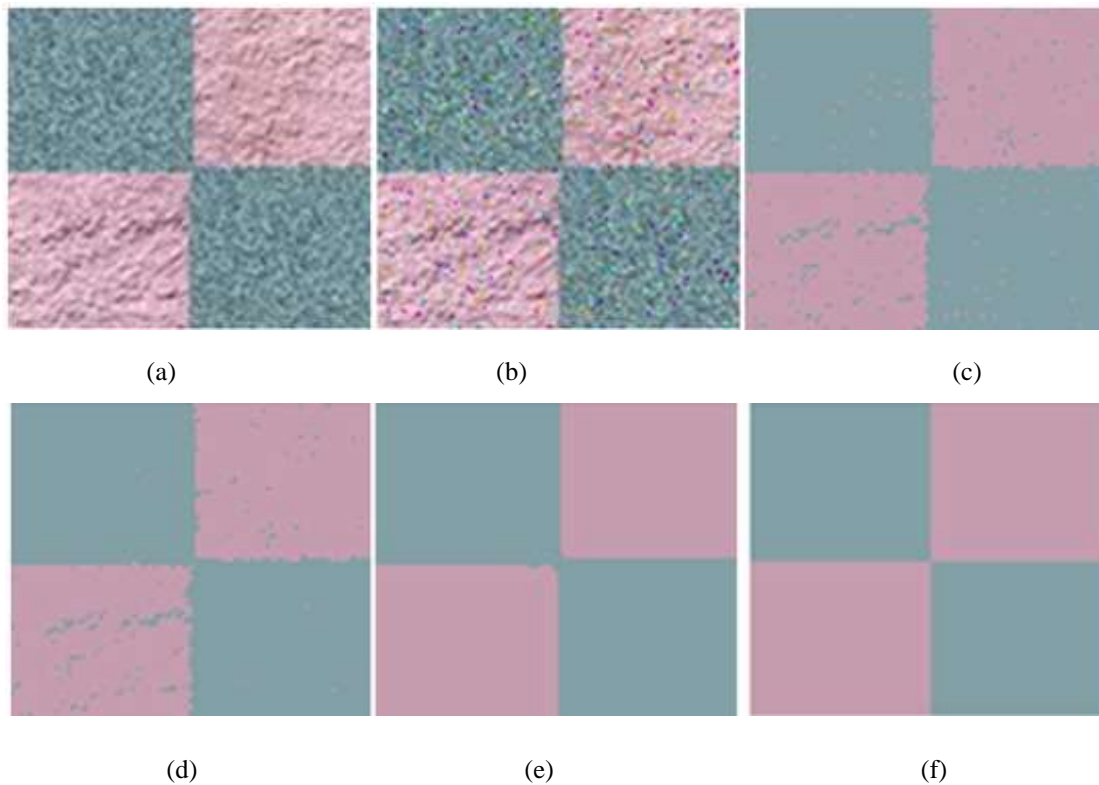
Fig. 7. Comparison of the proposed segmentation method with other existing methods on a synthetic image (2 classes). (a) Original image (256×256×3): color synthetic image with RGB description, (b) color synthetic image disturbed with a "salt and pepper" noise, (c) segmentation based on HCM and DS, (d) segmentation based on FCM and DS, (e) segmentation based on the proposed method, and (f) reference segmented image.

Table 2. Segmentation sensitivity From DDS, FCMDS, HHDS and TSMODS for the Data set Shown in Fig. 4

	HCMDS	FCMDS	PCMDS (THE PROPOSED METHOD)
	SENSITIVITY SEGMENTATION (%)		
Image 1	0.7938	0.8417	0.9860
Image 2	0.7717	0.8378	0.9944
Image 3	0.7909	0.8288	0.9781
Image 4	0.7381	0.7688	0.9683
Image 5	0.7148	0.7859	0.9779
Image 6	0.7358	0.7958	0.9898
Image 7	0.7340	0.7646	0.9831
Image 8	0.7450	0.8073	0.9834
Image 9	0.7302	0.8123	0.9766
Image 10	0.7004	0.7792	0.9843
Image 11	0.7636	0.8271	0.9834
Image 12	0.7512	0.8217	0.9751

In fact, the experimental segmentation results on medical and synthetic color images demonstrate the superiority of combining the second order statistics with the Possibilistic C-Means algorithm for the mass function estimation in the Dempster-Shafer evidence theory, as denoted by the segmentation sensitivity, see Table 1 and Table 2.

To evaluate the performance of the proposed segmentation algorithm, its accuracy was recorded. Regarding the accuracy, Tables 1 and 2 list the segmentation sensitivity of the different methods for the data set used in the experiment.

The segmentation sensitivity [31] [32] is computed using:

$$Sen\,(\%) = (\frac{N_{pcc}}{N \times M}) \times 100 \tag{19}$$

where Sens, Npcc, N×M are respectively the segmentation sensitivity (%), number of correctly classified pixels and dimension of the image.

The performance of the homogeneity method is quite acceptable. In fact, one can observe in Figures 7(c) and 7(d) that 20.62% and 15.83% of pixels were incorrectly segmented for the HCM and FCM methods, respectively.

However, this demonstrates that the mass functions resulting from the two algorithms, do not always correspond to the intuitive concept of degree of belonging or compatibility, and the generated mass functions do not have a typical interpretation. Moreover, the HCM and FCM algorithms are instable in noisy environments. However, errors were largely reduced when exploiting simultaneously the three images through the use of the DS fusion method including the homogeneity histogram.

Indeed, only 1.40% of pixels were incorrectly segmented in Figure 7(e). This good performance between these methods can also be easily assessed by visually comparing the segmentation results.

CONCLUSION

In this paper, we have proposed a new color image segmentation method for based on possibilistic C-means algorithm and Dempster-Shafer evidence theory. This method consists of two steps. In the first step, the automatic estimation of mass functions in the DS evidence theory is determined from the possibilistic C-means algorithm, which takes into account the compatibility information and the memberships resulting from this algorithm correspond to the intuitive concept of degree of belonging or compatibility. In the second step, the DS combination rule and decision are applied to fuse the six representative attribute images of the three primitive colors.

The proposed segmentation approach is conceptually different and explores a new strategy. In fact, instead of considering only one image for each application, many attribute images of the same image fused together may be very helpful to the segmentation process. The idea is to fuse one by one the pixels coming from different

information sources, in order to get a final reliable and accurate segmentation result.

The results obtained show the generic and robust character of the method in the sense that the model of the mass functions estimation in the DS evidence theory is appropriate. In image segmentation based on the DS evidence theory, the determination of mass functions is a hard task and the performance of the segmentation scheme is, however, largely conditioned by the appropriate determination of the mass functions, since assignation of a pixel to a cluster is given directly by the estimated mass functions.

The results obtained demonstrated the significant improved performance in segmentation. The proposed method can be useful for color image segmentation.

ACKNOWLEDGEMENTS

REFERENCES

1. Shih FY, Cheng S (2005) Automatic seeded region growing for color image segmentation. Image Vis. Comput. 23: 877-886.
2. Navon E, Miller O, and Averbuch A (2005) Color image segmentation based on adaptive local thresholds. Image and Vision Computing 23: 69-85.
3. Kwon MJ, Han YJ, Shin IH and Park HW (2003) Hierarchical fuzzy segmentation of brain MR images. Int. J. Imaging Systems and Technology 13: 115-125.
4. Chaabane SB, Sayadi M, Fnaiech F and Brassart E (2010) Colour image segmentation using homogeneity approach and data fusion techniques. EURASIP J. Adv. Signal Process 2010: 1-11.
5. Hao JT, Li ML and Tang FL (2008) Adaptive segmentation of cerebrovascular tree in time-of-flight magnetic resonance angiography. Medical & Biological Engineering & Computing 46: 75-83.
6. Michela G, Maurizio S, Silvia C, Beatrice A, Tommaso A and Claudio P (2012) Quantitative color analysis for capillaroscopy image segmentation. Medical & Biological Engineering & Computing 50: 567-574.
7. Harrabi R and Ben Braiek E (2011) Color image Segmentation using automatic thresholding techniques. SSD 2011: 1-6.
8. Chaabane SB and Fnaiech F (2014) Color edges extraction using statistical features and automatic thresholding technique: application to the breast cancer cells. Biomedical engineering Online 13: 1-18.
9. Liew AWC, Leung SH, and Lau WH (2000) Fuzzy image clustering incorporating spatial continuity. IEE Proc. Visual Image Signal Process. 147: 185-192.
10. Wyszecki G, Stiles WS (1982) Color Science: Concepts and Methods, Quantitative Data and formulae. John Wiley and Sons, second edition.
11. Ohta N (1977) Correspondance between ceilab and cieluv color differences. 2: 178-182.
12. Harrabi R and Ben Braiek E (2010) A comparative study of color image segmentation techniques using different color representation, JTEA, Tunisia 1-6.
13. Tkalcic M and Tasic JF (2003) Colour spaces: perceptual, historical and applicational background. IEEE EUROCON 1: 304-308.
14. Bloch I and Maitre H (1997) Fusion of image information under imprecision, in Aggregation and Fusion of Imperfect Information. Bouchon-Meunier Series Studies in Fuzziness Springer: 189-213.
15. Shafer G (1976) A Mathematical Theory of Evidence Princeton. University Press Princeton.
16. Bradley R (2007) A unified Bayesian decision theory. Theory and Decision, Springer US, 63: 233-263.
17. Shao-Long D, Jian-Ming W, Tao X and Hai-Tao L (2006) Constraint based Fuzzy Optimization Data Fusion for Sensor Network Localization. Second International Conference on Semantics Knowledge and Grid, SKG '06: 59-59.
18. Dubois D and Prade H (2003) Possibility theory and its applications: a retrospective and prospective view. The 12th IEEE International Conference on Fuzzy Systems: 5-11.
19. Denoeux T (1995) A k-nearest neighbour classification rule based on dempster-shafer theory. IEEE Trans. Syst. Man. and Cyber 25: 804-813.
20. Zhu YM, Dupuis O and Rombaut M (2002) Automatic determination of mass functions in Dempster-Shafer theory using fuzzy c-means and spatial neighborhood information for image segmentation. Opt. Eng. 41: 760-770.

21. *Vannoorenberghe P, Colot O and Brucq DD (1999) Color image segmentation using Dempster–Shafer's theory. Proc. ICIP'99: 300-304.*
22. *Lucas C and Araabi BN (1999) Generalization of the Dempster–Shafer theory: A fuzzy-valued measure. IEEE Trans. Fuzzy Syst. 7: 255-270.*
23. *Chaabane SB, Sayadi M, Fnaiech F and Brassart E (2008) Estimation of the mass function in the Dempster–Shafer's evidence theory using automatic thresholding for color image segmentation. International Conference on Signals, Circuits and Systems: 1-6.*
24. *Zimmerman HJ, Zysno P (1985) Quantifying vagueness in decision models. Eur. J. Oper. Res. 22: 148-158.*
25. *Bezdek JC (1981) Pattern Recognition with Fuzzy Objective Function Algorithms. Plenum, New York.*
26. *Duda Rand Hart P (1973) Pattern Classification and Scene Analysis. New York, Wiley.*
27. *Raghu K and Keller JM (1993) A possibilistic approach to clustering. IEEE Trans. Fuzzy Syst. 1: 98-110.*
28. *V Arvis, C Debain, M Berducat and A Benassi (2004) Generalization of the cooccurrence matrix for colour images: application to colour texture classification. Image Anal. Stereol 23: 63-72.*
29. *Clausi DA (2001) Comparison and fusion of cooccurrence, gabor and MRF texture features for classification of SAR sea-ice imagery. Atmosphere Ocean, 39: 183-194.*
30. *Harrabi R and Ben Braiek E (2012) Segmentation by Fusion of Histogram based on Dempster-Shafer Evidence Theory and Multi-level Thresholding in Different Color Spaces. EURASIP Journal on Image and Video Processing: 1-10.*
31. *Grau V, Mewes AUJ, Alcaniz M, Kikinis R, and Warfield SK (2004) Improved watershed transform for medical image segmentation using prior information. IEEE Transactions on Medical Imaging, 23: 447-458.*
32. *Duda RO, Hart PE, and Sork DG (2000) Pattern Classification. Wiley-Interscience, New York, NY, USA.*